Original Article

DEVELOPMENT OF AN 'OFF-THE-SHELF' GENE THERAPEUTIC NANOPARTICLE FORMULATION FOR INCORPORATION INTO BIOMATERIALS FOR REGENERATIVE MEDICINE APPLICATIONS

D.G. O'Shea[1,2], T. Hodgkinson[1,2,3], J.E. Dixon[4,5], C.M. Curtin[1,2,3] and F.J. O'Brien[1,2,3,*]

[1]Tissue Engineering Research Group, Department of Anatomy and Regenerative Medicine, RCSI University of Medicine and Health Sciences, D02 YN77 Dublin, Ireland
[2]Advanced Materials and Bioengineering Research Centre (AMBER), RCSI and TCD, D02 CP49 Dublin, Ireland
[3]Trinity Centre for Biomedical Engineering, Trinity College, D02 PN40 Dublin, Ireland
[4]Division of Regenerative Medicine & Cellular Therapies (RMCT), The University of Nottingham Biodiscovery Institute (BDI), School of Pharmacy, University Park, University of Nottingham, NG7 2RD Nottingham, UK
[5]NIHR Nottingham Biomedical Research Centre, University of Nottingham, NG7 2RD Nottingham, UK

Abstract

Traumatic musculoskeletal injuries require advanced therapeutic intervention to heal effectively. Regenerative medicine research has aimed to address this by using biomaterials to deliver gene therapeutic nanoparticles (NPs) to the injury site to direct healing. However, clinical translation has proven challenging due to the short shelf-life of NPs and requirements for cold storage conditions. Thus, this study aimed to investigate lyophilisation as a process to formulate 'off-the-shelf' NPs that can be incorporated into biomaterial scaffolds at the point of use and can be stored and transported at ambient temperatures. To this end, NPs consisting of a non-viral delivery vector, glycosaminoglycan-enhanced transduction (GET) peptide, complexed with plasmid DNA (pDNA), were formulated at three charge ratios (CRs - 6, 9, 12) and lyophilised. Firstly, the effects of lyophilisation on NP physicochemical properties were investigated; it did not affect NP size, polydispersity or charge. Next, the ability of the lyophilised NPs to express the pDNA cargo in mesenchymal stem cell (MSC) 2D monolayer culture was assessed. Transfection with lyophilised NPs at each CR promoted stable transgene expression and furthermore, once lyophilised, transgene expression could be maintained following long-term storage at room temperature. Transfection with lyophilised GET-pSOX9 NPs also significantly increased MSC-mediated articular cartilage matrix deposition in methacrylated hyaluronic acid (MeHA)-collagen type II (Col II) injectable hydrogel scaffolds, highlighting the therapeutic potential of this NP formulation. In conclusion, this study outlines an effective method for formulating 'off-the-shelf' NPs for regenerative medicine applications that could be applied to the musculoskeletal system as well as other tissues.

Keywords: Regenerative medicine, gene therapy, non-viral gene delivery, lyophilisation, gene-activated scaffolds, gene-activated hydrogels.

***Address for correspondence**: Prof. Fergal J. O'Brien, Tissue Engineering Research Group (TERG), RCSI University of Medicine and Health Sciences, 123 St. Stephen's Green, Dublin 2, Ireland. Email: fjobrien@rcsi.ie

Introduction

Gene therapy is a novel approach to personalised medicine that aims to up-regulate or silence gene expression in cells to achieve a specific therapeutic aim. This is achieved by complexing a genetic cargo to a suitable delivery vector to form gene therapeutic nanoparticles (NPs) that can then be administered directly to the patient, or used to modify extracted cells *ex vivo* that can then be re-introduced into the patient (Bulaklak and Gersbach, 2020; Collins *et al.*, 2023; U.S. Food and Drug Administration, 2018). Gene therapy has revolutionised the field of regenerative medicine by providing a means to promote repair of a wide range of traditionally difficult to target tissues without the need for high doses of exogenous growth factors (Bleiziffer *et al.*, 2007; Kelly *et al.*, 2019).

Articular cartilage (AC) is an example of one conventionally difficult to repair tissue in the field of regenerative medicine, which has the potential to benefit from gene therapy interventions. Existing surgical procedures for the treatment of AC defects can lead to variable healing and

the deposition of mechanically inferior fibrocartilage, and so novel treatment strategies are required (Hodgkinson *et al.*, 2022a; Hodgkinson *et al.*, 2022b; Kwon *et al.*, 2019; O'Brien, 2011; Pelttari *et al.*, 2008; Steadman *et al.*, 2003). Recent research in this field has aimed to promote cartilage repair by functionalising biomaterial scaffolds and hydrogels with cells, such as bone marrow derived mesenchymal stem cells (MSCs) (Kajave *et al.*, 2020; Liang *et al.*, 2022; Luo *et al.*, 2020; Ni *et al.*, 2020). However, challenges remain in stimulating and maintaining differentiation of MSCs to AC-like phenotypes and preventing these cells from following a fibrocartilage lineage (Yang *et al.*, 2020). The composition of the biomaterial scaffold or hydrogel can help to direct MSC differentiation, and it has been shown that human AC-inspired biomaterials such as hyaluronic acid (HA) and collagen type II (Col II) can promote chondrogenesis (Erickson *et al.*, 2009; Hauptstein *et al.*, 2020; Intini *et al.*, 2022a; Intini *et al.*, 2022b; Kilmer *et al.*, 2020; O'Shea *et al.*, 2022; O'Shea *et al.*, 2024; Yuan *et al.*, 2016). However, to maintain articular phenotypes in differentiated MSCs while directing effective healing of the tissue, additional therapeutic intervention is required. Therefore, growth factors such as those from the transforming growth factor beta (TGF-β) family and the bone morphogenetic protein (BMP) family, amongst others, have been used to enhance the chondrogenic differentiation of MSCs (Chen *et al.*, 2020; Hauptstein *et al.*, 2022; Puiggalí-Jou *et al.*, 2023; Wang *et al.*, 2021; Yang *et al.*, 2021). However, growth factor doses far in excess of physiological concentrations are required to promote healing in scaffolds and hydrogels, which may lead to off-target side-effects in patients (Chen *et al.*, 2010; Freeman *et al.*, 2020; Kelly *et al.*, 2019; Laird *et al.*, 2021). Other strategies target transcription factors such as members of the SOX family (SOX5, SOX6 and SOX9) which have been shown to be master regulators of cartilage formation (Green *et al.*, 2015). However, delivery of these factors into cells can prove challenging due to their physicochemical properties (Rilo-Alvarez *et al.*, 2021). Gene therapy offers a promising alternative as nucleic acids, such as plasmid DNA (pDNA), could be used to induce local expression of these therapeutic proteins in patient cells, negating the need for administration of high doses of exogenous growth factors (Gonzalez-Fernandez *et al.*, 2016; Jeon *et al.*, 2012; Laird *et al.*, 2021; Liu *et al.*, 2023).

One challenge in the field is that primary cells used in articular cartilage repair, such as MSCs and chondrocytes, are notoriously challenging to transfect and so an effective delivery vector is required to transport the nucleic acid cargo into the cell (Hamm *et al.*, 2002). Viral delivery vectors have been commonly used in this space, however non-viral alternatives such as lipid NPs, polymers and cell-penetrating peptides (CPPs) are becoming increasingly popular in the field due to safety concerns associated with viral vectors (Dunbar *et al.*, 2018; Guo and Huang, 2012; Kelly *et al.*, 2019). In particular, CPPs such as the glycosaminoglycan binding enhanced transduction (GET) peptide have displayed potential for cartilage repair applications due to their biocompatibility and their ability to transfect primary cells, including MSCs (Dixon *et al.*, 2016; Joyce *et al.*, 2024; Thiagarajan *et al.*, 2017). The GET peptide consists of three domains - a 16-residue heparan sulphate-GAG binding peptide derived from the fibroblast growth factor 2 (FGF2) protein (FGF2B) to stimulate cell interaction; an amphiphilic pan-nucleic acid interaction sequence (LK15); and 8 arginine (8R) to facilitate cell entry (Dixon *et al.*, 2016). The GET peptide demonstrates relatively high transfection efficiency, low toxicity and can be used to transport a variety of nucleic acid cargoes into primary cells (Dixon *et al.*, 2016; Dixon *et al.*, 2024; Raftery *et al.*, 2019). Therefore, the GET peptide was chosen as the delivery vector for this study.

Gene therapeutic NPs could also be incorporated into hydrogels for cartilage repair applications to form 'gene-activated hydrogels'. This method of gene delivery is potentially advantageous as the hydrogel offers additional protection to the nucleic acid cargo and, if designed with appropriate properties, can be administered directly into the injury site via minimally invasive arthroscopic injection. This would help to reduce the risk of off-target side-effects for patients (Biondi *et al.*, 2008; Municoy *et al.*, 2020). A number of research groups have investigated the use of hydrogels as a platform for gene delivery to injured articular cartilage and have reported enhanced regeneration *in vitro* and *in vivo* when compared to gene-free hydrogel controls (Chen *et al.*, 2023; Lolli *et al.*, 2019; Madry *et al.*, 2020a; Maihöfer *et al.*, 2021). In our own lab, collagen and glycosaminoglycan-based scaffolds have been investigated as a platform to deliver non-viral gene therapeutic NPs for a range of applications including bone repair (Curtin *et al.*, 2015; Power *et al.*, 2022; Raftery *et al.*, 2018; Raftery *et al.*, 2019; Walsh *et al.*, 2021) and cartilage repair (Intini *et al.*, 2023; Raftery *et al.*, 2020), amongst other applications. However, despite the potential advantages of using gene-activated hydrogels for cartilage repair, clinical translation of these products may prove challenging due to the short shelf-life of gene therapeutic NPs. Complexation of gene therapeutic NPs immediately prior to use in a clinical setting may be impractical for the clinician and introduces the risk of batch-to-batch variability. This method of NP preparation would also make quality testing of the final product challenging and may not comply with good manufacturing practice (GMP). Therefore, a method of formulating these NPs for stable long-term stable storage and easy reconstitution at point of application would be very beneficial to clinical translation.

To this end, a number of research groups have investigated methods of extending the shelf-life of gene therapeutic NPs through the use of techniques such as freezing, spray drying and lyophilisation (Keil *et al.*, 2019; Veilleux

et al., 2016; Zhao *et al.*, 2020). Lyophilisation is a technique that is of particular interest as it is used extensively in the pharmaceutical industry in the preparation of stable drug formulations and involves the removal of water content from a formulation via sublimation (Bjelošević *et al.*, 2020). Thus, the overarching aim of this study was to investigate lyophilisation as a process to enable stable storage of GET-pDNA NPs as an 'off-the-shelf' formulation for use in regenerative medicine applications. Lyophilisation has successfully been used by a number of research groups to prepare stable formulations of polyethylenimine (PEI)-pDNA NPs (Hahn *et al.*, 2010), RALA-pDNA NPs (Cole *et al.*, 2018), chitosan-pDNA NPs (Veilleux *et al.*, 2016), lipid-siRNA and lipid-mRNA NPs (Ball *et al.*, 2017; Zhao *et al.*, 2020), amongst others. However, to our knowledge, a lyophilised non-viral delivery vector and nucleic acid NP formulation for incorporation into hydrogels for articular cartilage repair has yet to be developed. Therefore in this study, it was hypothesised that lyophilisation would enable stable storage of GET-pDNA NPs at room temperature, without negatively impacting NP physicochemical properties or transgene expression following transfection. To test this hypothesis, the effects of lyophilisation on GET-pDNA NP physicochemical properties were first assessed. Following this, the ability of these NPs to express their pDNA cargo in MSCs in 2D monolayer was investigated and pDNA expression following long-term storage of the NPs was also assessed. Subsequently, with cartilage in mind as an exemplar clinical indication, and a view to future studies, therapeutic (SOX9) pDNA cargoes which have proven chondrogenic capacity were investigated and the ability of lyophilised GET-pSOX9 NPs to promote MSC-mediated AC matrix deposition in methacrylated hyaluronic acid (MeHA)/Col II injectable hydrogel scaffolds was determined.

Materials and Methods

Nanoparticle Formulation

Plasmid Propagation and GET Peptide Synthesis

Propagation of plasmids containing the *Gaussia luciferase* (pGLuc; New England BioLabs, MA, USA) and human sex-determining region Y-box 9 (SOX9) (pSOX9; Origene Technologies, MD, USA) gene were carried out respectively. The pGLuc and pSOX9 plasmids contained the cytomegalovirus (CMV) promoter and expressed ampicillin resistance genes. Propagation of plasmids was carried out by transforming into One Shot™ TOP10 chemically competent *E. coli* (ThermoFisher Scientific, Dublin, Ireland) cells as per the manufacturer's instructions. The transformed *E. coli* cells were subsequently cultured in lysogeny broth (LB; Sigma Aldrich, Wicklow, Ireland) containing 100 µg/mL ampicillin (Fisher Scientific, Dublin, Ireland). pDNA was isolated and purified using a PureLink™ Expi Endotoxin-Free Mega Plasmid Purification Kit (ThermoFisher Scientific, Dublin, Ireland), diluted in molecular grade water (MGH_2O; Sigma Aldrich, Wicklow, Ireland) and stored at – 20 °C.

GET peptides were synthesised using solid phase t-Boc chemistry and purified to >90 % by Protein Peptide Research Ltd (PPR, Fareham, UK), as previously described (Osman *et al.*, 2018; Spiliotopoulos *et al.*, 2019).

Freshly Complexed GET-pDNA Nanoparticle Formulation

GET-pDNA nanoparticles (NPs) were formulated at previously optimised charge ratios (CRs - the ratio of positively charged peptide to negatively charged pDNA) of 6, 9 or 12, as described by our research group (Joyce *et al.*, 2024; Power *et al.*, 2022; Raftery *et al.*, 2019). Briefly, to formulate NPs at CR 6 composing 1 µg pDNA, 1 µL of 1 mM GET peptide and 1 µL of 1 µg/µL pGLuc were each diluted in 12.5 µL MGH_2O in pyrogen-free 1.5 mL Eppendorf tubes. The diluted GET peptide was then added to the diluted pDNA (1:1 ratio of GET:pDNA) and the solutions were mixed by gently tapping the bottom of the Eppendorf tube. Nanoparticle complexation was then allowed to occur for 15mins at room temperature. This procedure was repeated using 1:1.5 and 1:2 ratios of GET:pDNA to formulate NPs at CR 9 and CR 12 respectively.

Lyophilised GET-pDNA Nanoparticle Formulation

Freshly complexed GET-pDNA NPs were formulated at CR 6, 9 or 12 as outlined above. The NP solutions were then diluted in a 3:1 ratio with 20 % (w/v) trehalose (Sigma Aldrich, Wicklow, Ireland), which served as a cryoprotectant (Trenkenschuh and Friess, 2021). The NPs were then lyophilised in a Christ Epsilon benchtop freeze dryer (Martin Christ, Osterode am Harz, Germany) using a lyophilisation cycle adapted from that outlined by Cole *et al.* (2018). Briefly, the NPs underwent freezing at – 40 °C for 1hr, primary drying at – 40 °C and 120 mTorr for 3 hrs, – 30 °C and 190 mTorr for 4 hrs and then 25 °C and 190 mTorr for 4 hrs. Finally, the NP samples underwent secondary drying at 20 °C and 190 mTorr for 18 hrs and 20 °C and 50 mTorr for a further 10 hrs. Lyophilised NPs were stored at room temperature, protected from light.

Nanoparticle Physicochemical Characterisation

Nanoparticle Size, Polydispersity Index and Zeta Potential

Freshly complexed and lyophilised GET-pGLuc NPs at CR 6, 9 and 12 were formulated as described above and diluted to a concentration of 2 µg/mL pDNA using MGH_2O. 1 mL of each NP solution was then transferred to a DTS1070 Malvern Zetasizer capillary cell using a 1 mL Luer slip syringe (Fisher Scientific, Dublin, Ireland). NP size, which is measured as mean NP hydrodynamic diameter, and polydispersity, which is a measure of NP size distribution, were assessed via dynamic light scattering using the Malvern Instruments Zetasizer 3000 HS (Malvern Panalytical Ltd., Malvern, UK). NP zeta potential, which is a measure of NP surface charge, was assessed via elec-

trophoretic light scattering also using the Malvern Instruments Zetasizer 3000 HS.

pDNA Encapsulation Efficiency

Encapsulation efficiency is a measure of the percentage of available pDNA that is bound by the delivery vector to form NPs. In this study, encapsulation efficiency was qualitatively assessed using agarose gel electrophoresis and the percentage encapsulation efficiency was quantitatively determined using the Promega QuantiFluor® double-stranded DNA (dsDNA) system (MyBio Ltd., Kilkenny, Ireland). To conduct the agarose gel electrophoresis, freshly complexed and lyophilised GET-pGLuc NPs at CR 6, 9 and 12 were formulated as described above and diluted to a concentration of 12 µg pDNA per mL using MGH_2O. A 1 % agarose gel was then prepared in 1X tris-borate-EDTA (TBE) buffer containing 1× SYBR Safe DNA gel stain (ThermoFisher Scientific, Dublin, Ireland). 5 µL of each sample was added to 20 µL MGH_2O and 5 µL TriTrack 6× DNA loading dye (ThermoFisher Scientific, Dublin, Ireland), and 20 µL of each sample-dye solution was added to the wells of the 1 % agarose gel. A 1 kB DNA ladder and pGLuc alone were also added as controls. The gel was run at 80 V for 1hr and subsequently viewed under a UV transilluminator and imaged using Syngene Genesnap techonology.

The Promega QuantiFluor® dsDNA system assay was conducted as outlined by Power *et al.* (2022). Briefly, freshly complexed and lyophilised GET-pGLuc NPs at CR 6, 9 and 12 were formulated as described above and diluted to a concentration of 10 µg pDNA per mL using MGH_2O. 10 µL of each formulation was subsequently pipetted in duplicate into the wells of a black 96-well polystyrene plate and 200 µL of the QuantiFluor® dsDNA fluorescent binding dye was added to each well, as per manufacturer's instructions. pGLuc only at a concentration of 10 µg/mL was employed as a positive control and MGH_2O was utilised as the negative control. The plate was read on a Tecan Infinite® 200 Pro plate reader (Tecan, Männedorf, Switzerland) (excitation wavelength 504 nm, emission wavelength 531 nm) and encapsulation efficiency was determined by expressing the fluorescence of each sample as a percentage of the fluorescence of the pDNA only control.

Rat Mesenchymal Stem Cell Isolation and Culture

Mesenchymal stem cells (MSCs) were extracted from the bone marrow of 6 to 8 week old female Sprague Dawley rats, as approved by the Research Ethics Committee of the Royal College of Surgeons in Ireland under application number REC202012003, as previously described (O'Shea *et al.*, 2024; Power *et al.*, 2022). Briefly, the bone marrow of the femurs of both hind limbs of the animals were flushed out with growth medium (high glucose Dulbeccos's Modified Eagle Medium (DMEM) containing 20 % (v/v) foetal bovine serum (FBS), 2 % (v/v) penicillin streptomycin antibiotics, 0.002 % (v/v) primocin, 1 % (v/v) GlutaMAX and 1 % (v/v) non-essential amino acids). The isolate was incubated at 37 °C and 5 % CO_2 in growth medium for 24 hrs, before being centrifuged at 300 ×*g* for 5 mins. The resultant cell pellet was resuspended in growth medium and cells were cultured at 37 °C and 5 % CO_2 until passage 5 for transfection experiments.

Determination of Lyophilised GET-pDNA Nanoparticle Transfection Efficiency in 2D Monolayer

Transfection of MSCs with Lyophilised GET-pDNA Nanoparticles

MSCs at passage 5 were seeded in monolayer at a density of 2.5 × 10^4 cells per well on a tissue culture-treated plastic 12-well plate 24 hrs prior to transfection and the cell media in the well plate was changed immediately prior to transfection. Freshly complexed GET-pGLuc NPs were formulated in Opti-MEM™ (ThermoFisher Scientific, Dublin, Ireland) as outlined above. Lyophilised GET-pDNA NPs at CR 6, 9 and 12 were formulated as outlined above and reconstituted within 7 days of lyophilisation in 75 µL Opti-MEM™. 25 µL freshly complexed NPs or reconstituted NP lyophilate (equivalent to 1 µg pDNA) were then added directly to the cell media in the appropriate wells of the 12-well plates.

Assessment of Cell Viability Post-Transfection

An alamarBlue assay (Biosciences, Dublin, Ireland) was used to assess cell metabolic activity at 3, 7 and 10 days post-transfection, as per the manufacturer's instructions. In short, the alamarBlue reagent was mixed 1 in 10 with GM and 300 µL of the diluted reagent was then added to the individual wells of the 12-well plates. The 12-well plates were then covered with tinfoil and incubated at 37 °C for 1 hr. Subsequently, two 90 µL aliquots were pipetted from each well into a black polystyrene 96-well plate and the fluorescence of the reduced alamarBlue reagent was analysed using a Tecan Infinite® 200 Pro plate reader (excitation wavelength 545 nm, emission wavelength 590 nm). The metabolic activity of the transfected cells was then calculated as a percentage of the metabolic activity of the non-treated cell controls.

Assessment of Nanoparticle Transfection Efficiency

To assess NP transfection efficiency, cell media samples were collected from the 12-well plates at 3, 7 and 10 days post-transfection and assessed for the presence of *Gaussia luciferase* using a Pierce™ Gaussia Luciferase Flash Assay Kit (ThermoFisher Scientific, Dublin, Ireland). *Gaussia luciferase* is a luminescent reporter protein that is secreted into the cell media if the transfection is successful. The assay was carried out according to the manufacturer's instructions. Briefly, two 20 µL aliquots of each media sample were pipetted into a black polystyrene 96-well plate. Subsequently, 100× coelenterazine was diluted

in a 1:100 ratio with 1× tris-EDTA (TE) buffer and 100 µL of this working solution was added to each well. Luminescence was then analysed immediately on a Tecan Infinite® 200 Pro plate reader at 485 nm.

Determination of Lyophilised GET-pDNA Nanoparticle Transfection Efficiency Following Long-Term Storage at Room Temperature

Transfection experiments were carried out using GET-pGLuc NPs at CR 6, 9 and 12 that had been stored at room temperature in sealed glass vials and protected from light for 1 month, 3 months and 6 months respectively, as outlined in Transfection of MSCs with lyophilised GET-pDNA nanoparticles. Cell viability was assessed post-transfection by measuring cell metabolic activity, as outlined in Assessment of cell viability post-transfection. NP transfection efficiency was determined by measuring the relative luminescence of *Gaussia luciferase* in the media, as outlined in Assessment of nanoparticle transfection efficiency.

Determination of the Ability of Lyophilised GET-pSOX9 Nanoparticles to Induce Chondrogenic Differentiation of MSCs in 3D Culture in Hydrogel Scaffolds

Synthesis of Methacrylated Hyaluronic Acid

Methacrylated hyaluronic acid (MeHA) was synthesised via reaction of hyaluronic acid (HA) with methacrylic anhydride at a 1:3 molar ratio, as previously outlined (O'Shea *et al.*, 2024). Briefly, hyaluronic acid sodium salt (HA; MW 1.5-1.8 × 106 Da, from Streptococcus equi, Sigma Aldrich, Wicklow, Ireland) was dissolved in deionised water to a concentration of 1 % (w/v). Subsequently, an equal volume of N,N-dimethlyformamide (DMF; Sigma Aldrich, Wicklow, Ireland) was added dropwise. Methacrylic anhydride (MA; Sigma Aldrich, Ireland) was added at a HA disaccharide unit: MA molar ratio of 1:3 while maintaining the pH at 8 to 9 using 5 M sodium hydroxide (NaOH; ThermoFisher Scientific, Dublin, Ireland). After overnight stirring at 2 to 8 °C, sodium chloride (NaCl; ThermoFisher Scientific, Dublin, Ireland) was added to a final concentration of 0.5 M. The synthesised MeHA was then precipitated by adding a 1.5× volume of 100 % (v/v) ethanol, and then transferred to a dialysis membrane (SnakeSkin™ Dialysis Tubing, 10K MWCO, ThermoFisher Scientific, Dublin, Ireland) and dialysed against deionised water for 5 days. The MeHA was then lyophilised over 48 hrs using a FreeZone benchtop freeze-dryer (Labconco, MO, USA). The purified MeHA, with a 23 ± 1 % degree of HA functionalisation (as determined by proton nuclear magnetic resonance (^{1}H-NMR) from an average of 3 batches), was stored at – 20 °C prior to reconstitution.

Formulations of MeHA-Collagen Type II Injectable Hydrogel

A MeHA-collagen type II (Col II) injectable hydrogel was formulated as previously described (O'Shea *et al.*, 2024). Briefly, MeHA was dissolved to a concentration of 2.4 % (w/v) in a photoinitiator solution composed of 0.1 % (w/v) lithium phenyl-2,4,6-trimethylbenzoylphosphinate (LAP; Sigma Aldrich, Wicklow, Ireland) in sterile phosphate buffered saline (PBS; Sigma Aldrich, Wicklow, Ireland). The 2.4 % (w/v) MeHA hydrogel was mixed in a 1:1 ratio with a 2.4 % (w/v) neutralised Col II hydrogel (prepared from porcine knee cartilage, Symatese, Vourles, France) using two coupled 5 mL syringes to yield a 1.2 % (w/v) MeHA and 1.2 % (w/v) Col II hydrogel.

Monolayer Transfection of Pre-Transfected Mesenchymal Stem Cells

Monolayer transfection of pre-transfected MSCs was conducted using a protocol adapted from that previously outlined by Gonzalez-Fernandez *et al.* (2019). Briefly, MSCs at passage 4 were seeded in T175 flasks at a density of 1 × 10^6 cells per flask and cultured for 3 days in growth medium. Freshly complexed and lyophilised GET-pSOX9 NPs were formulated at CR 6 as outlined above and diluted in growth medium such that 10 mL of medium contained 20 µg pDNA. For the transfection, the medium was removed from each flask and replaced with 10 mL freshly complexed or lyophilised NP-containing medium. The flasks were then incubated at 37 °C for 1 day before the NP-containing medium was removed and replaced with fresh growth medium for a further 3 days.

Preparation and *in Vitro* Culture of Gene-Activated Hydrogel Scaffolds

The pre-transfected MSCs were trypsinised and re-suspended in incomplete chondrogenic medium (ICM; 0.005 % (w/v) 2-phospho-L-ascorbic acid, 0.004 % (w/v) L-proline, 100 nM dexamethasone, 1 % (v/v) sodium pyruvate, 1 % (v/v) insulin-transferrin-selenium-ethanolamine (ITS-X), 1 % (v/v) GlutaMAX and 0.002 % (v/v) primocin in high glucose DMEM) such that 200 µL of ICM contained 6 × 10^6 cells. Cell suspension (200 µL) was subsequently incorporated into 1 mL of hydrogel using two coupled 5 mL syringes to yield a 1 % (w/v) MeHA and 1 % (w/v) Col II hydrogel containing pre-transfected cells at a density of 5 × 10^6 cells per mL of hydrogel. Injectable scaffolds were then fabricated by injecting the cell incorporated hydrogel into 6 mm × 5 mm Teflon moulds, followed by photocrosslinking with blue light (405 nm) for 2 mins. The cell incorporated scaffolds were incubated at 37 °C and 5 % CO_2 in complete chondrogenic medium (CCM; ICM with 20 ng/mL recombinant human TGF-β3 (PeproTech, London, UK)) for 28 days.

Quantification of Sulfated Glycosaminoglycan Deposition by Mesenchymal Stem Cells

Subsequently, the sulfated glycosaminoglycan (sGAG; a constituent of AC extracellular matrix) content of the MeHA-Col II injectable scaffolds was quantified using a Blyscan Sulfated Glycosaminoglycan Assay kit

(Biocolor Life Sciences, Antrim, UK), as previously described (O'Shea *et al.*, 2024). Briefly, the hydrogel scaffolds were digested in papain enzyme solution (PBS containing 0.4 % (w/v) ethylenediaminetetraacetic acid (EDTA; Sigma Aldrich, Wicklow, Ireland), 0.8 % (w/v) sodium acetate (Sigma Aldrich, Wicklow, Ireland), 0.08 % (w/v) L-cysteine hydrochloride (Sigma Aldrich, Wicklow, Ireland) and 0.01 % (w/v) papain enzyme (Carica papaya; Sigma Aldrich, Wicklow, Ireland)) at 60 °C overnight. Dye reagent (1 mL) was then added to 100 µL of each sample and standard and incubated at room temperature with gentle agitation for 30 mins. The samples were then centrifuged at 12,000 rpm for 10 mins and the supernatant was removed. Dissociation reagent (0.5 mL) was subsequently added to each sample and standard and vortexed to dissolve the sGAG-bound dye. 200 µL of each sample and standard was then added in duplicate to the wells of a clear 96-well plate and absorbance was read at 656 nm using a Tecan Infinite® 200 Pro plate reader. sGAG quantity was determined from a standard curve.

The amount of double-stranded DNA (dsDNA) in the scaffolds was also assessed, as an indication of cell quantity, with a Quant-iT PicoGreen dsDNA kit (Biosciences, Dublin, Ireland), according to the manufacturer's protocol. Fluorescence of the samples was measured at an excitation wavelength of 485 nm and an emission wavelength of 538 nm using a Tecan Infinite® 200 Pro plate reader and dsDNA quantity was determined from a standard curve.

Histological Analysis of Sulfated Glycosaminoglycan Deposition

Scaffolds were treated with 30 % (w/v) sucrose, embedded in Optimal Cutting Temperature (OCT) medium (ThermoFisher Scientific, Dublin, Ireland) and sectioned into 7 µm thick sections using a Leica CM1950 cryostat (Leica, Wetzlar, Germany), as previously described (O'Shea *et al.*, 2024). The sections were then mounted on Superfrost™ Plus microscope slides (Epredia, Runcorn, UK) and the OCT was removed and the sections were hydrated in deionised water in preparation for staining. Weigert's haematoxylin (stains nuclei black/dark purple; Sigma Aldrich, Wicklow, Ireland), safranin-O (stains sGAG red; Sigma Aldrich, Wicklow, Ireland) and fast green (provides a light counterstain; Sigma Aldrich, Wicklow, Ireland) were used to stain the sections. Finally, the sections were dehydrated in 95 % (v/v) ethanol, 100 % (v/v) ethanol and xylene and mounted using DPX (Sigma Aldrich, Ireland) and coverslips. Sections were subsequently imaged at 4× magnification using a Nikon Eclipse 90i microscope (Nikon Instruments Inc., NY, USA).

Immunohistochemical Analysis of Collagen Type I and Collagen Type II Deposition

Immunohistochemistry (IHC) staining was used to detect the presence of collagen type I (Col I) and Col II, as previously described (Joyce *et al.*, 2023; O'Shea *et al.*, 2024). Col I deposition indicates the formation of fibrocartilage, while Col II deposition indicates the formation of an AC-like matrix by the cells. Briefly, endogenous peroxidase activity was inhibited using 0.3 % (v/v) hydrogen peroxide (Abcam, Cambridge, UK) and the sections were then blocked with IHC blocking buffer (1 % (w/v) bovine serum albumin (Sigma Aldrich, Wicklow, Ireland) and 5 % (v/v) goat serum (Abcam, UK) in PBS). Sections were treated with mouse primary antibodies for COL-1 (ab6308, Abcam, Cambridge, UK) or COL-2 (SC52658, Santa Cruz, USA) at 1:200 and 1:100 dilutions, respectively, overnight. The next day, sections were exposed to a 1:500 dilution of HRP-conjugated goat anti-mouse IgG secondary antibody (ab6728, Abcam, UK), and the target antigen signal was amplified using an avidin/biotin-based peroxidase system (PK-6101, Vector Laboratories, CA, USA). Finally, the sections were incubated in 3,3′-diaminobenzidine (DAB) (Vector Laboratories, CA, USA).

Statistical Analysis

Quantitative data collected in this study was analysed using Excel (2016, Microsoft, WA, USA) and Prism (8.0.1, GraphPad, MA, USA) software. Two-way Analysis of Variance (ANOVA) with Tukey post hoc analysis was employed when investigating the impact of two independent variables on a dependent variable, while one-way ANOVA with Tukey post hoc analysis was used when assessing the influence of one independent variable on a dependent variable. Physicochemical characterisation experiments involved the analysis of n = 3 samples, 2D transfection experiments were repeated n = 3 times, and 3D transfection experiments were conducted on n = 4 scaffolds.

Results

Lyophilisation of GET-pDNA Nanoparticles Does not Affect Physicochemical Properties

Lyophilised GET-pDNA nanoparticles (NPs) at CR 6, 9 and 12 were first assessed to determine if the lyophilisation process had an effect on their physicochemical properties when compared to freshly complexed NPs at the same CR. Lyophilisation did not result in any significant change in NP diameter, with both freshly complexed and lyophilised NPs at all CRs displaying mean diameters of approximately 150 nm (Fig. 1**a**). Polydispersity index (PdI) is a measure of the size distribution of the NP sample and values range from 0 for a uniform sample, to 1 for a highly polydisperse sample (Danaei *et al.*, 2018). Similar to NP size, lyophilisation did not result in a significant change in NP PdI when compared to freshly complexed NPs at the same CR (Fig. 1**b**). Likewise, there was no significant change in NP surface charge following lyophilisation at each CR with surface charge values ranging from approximately 30 to 40 mV, dependent on CR (Fig. 1**c**).

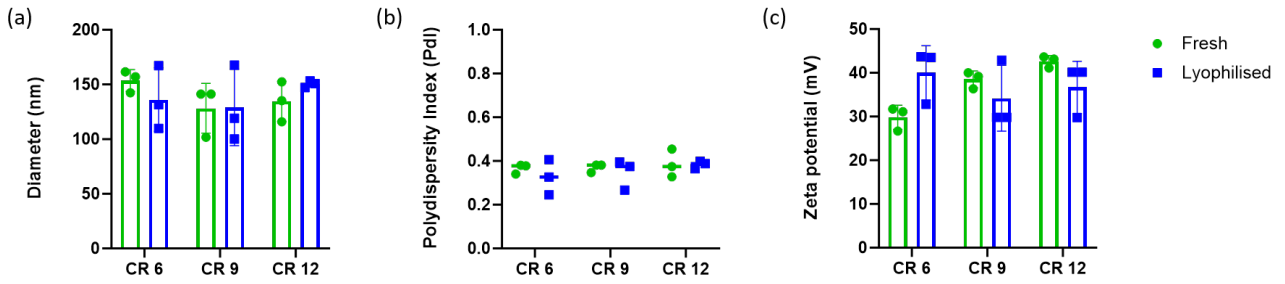

Fig. 1. Physicochemical analysis of the lyophilised GET-pDNA NPs. There was no statistically significant difference in (**a**) size, (**b**) polydispersity or (**c**) surface charge between lyophilised NPs and freshly complexed NP controls. Error bars represent ± SD, *n* = 3 samples tested. GET, glycosaminoglycan-enhanced transduction; pDNA, plasmid DNA; NPs, nanoparticles.

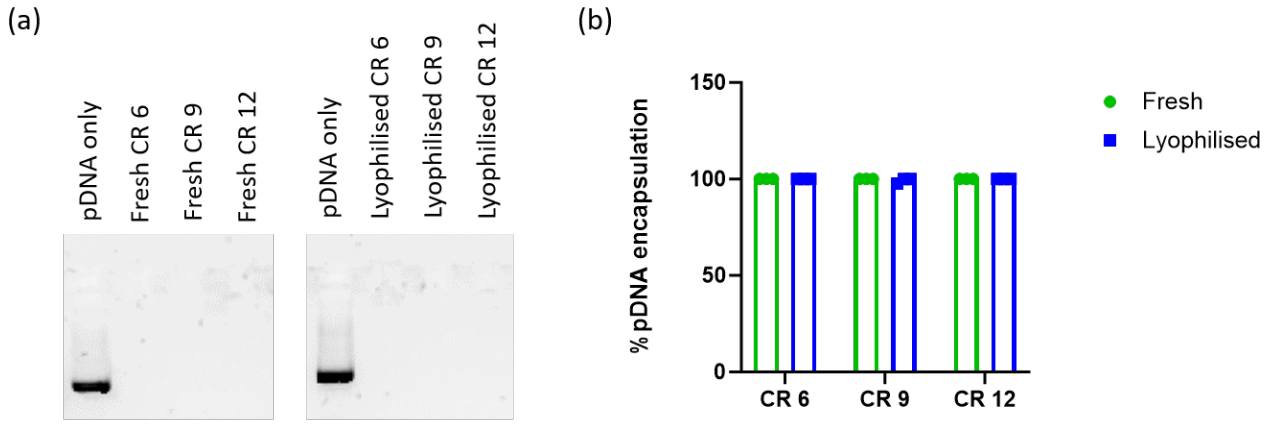

Fig. 2. Assessment of the percentage pDNA encapsulation within freshly complexed and lyophilised GET-pDNA NPs at CR 6, 9 and 12. 100 % of the pDNA was encapsulated within the NP as demonstrated using (**a**) gel electrophoresis and (**b**) a Quantifluor® dsDNA system assay. Error bars represent ± SD, *n* = 3 samples tested. CR, charge ratio.

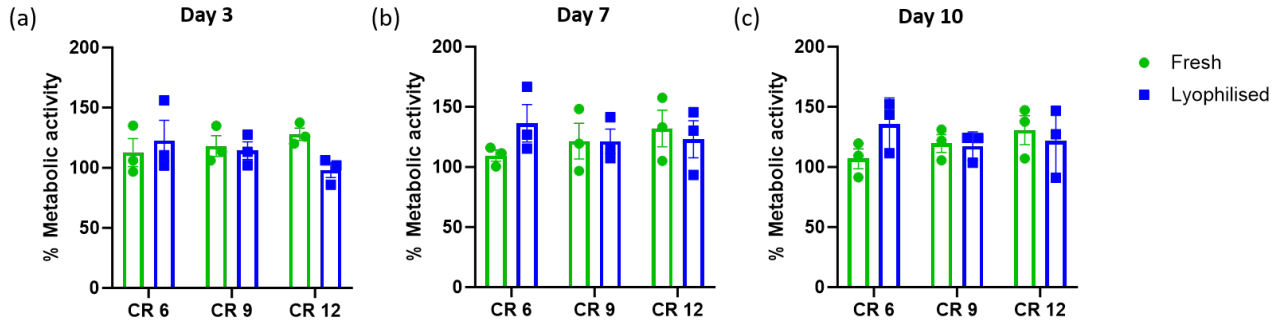

Fig. 3. Cell metabolic activity of MSCs post-transfection with lyophilised GET-pDNA NPs. There was no statistically significant difference in cell metabolic activity, normalised to non-treated cell controls, between cells transfected with freshly complexed and lyophilised NPs respectively at (**a**) 3, (**b**) 7 and (**c**) 10 days post-transfection indicating that the NPs were non-toxic to the cells. Error bars represent ±SE, *n* = 3 repeats. MSCs, mesenchymal stem cells.

Lyophilisation of GET-pDNA Nanoparticles Does not Affect pDNA Encapsulation Efficiency

Agarose gel electrophoresis was used to determine if there was any unbound pDNA present following NP complexation and showed that the pDNA was completely encapsulated in both the freshly complexed and lyophilised NPs (Fig. 2**a**). The Quantifluor® dsDNA stain was used to quantify these results and showed that >98 % pDNA was encapsulated in both the freshly complexed and lyophilised NPs at each CR (Fig. 2**b**).

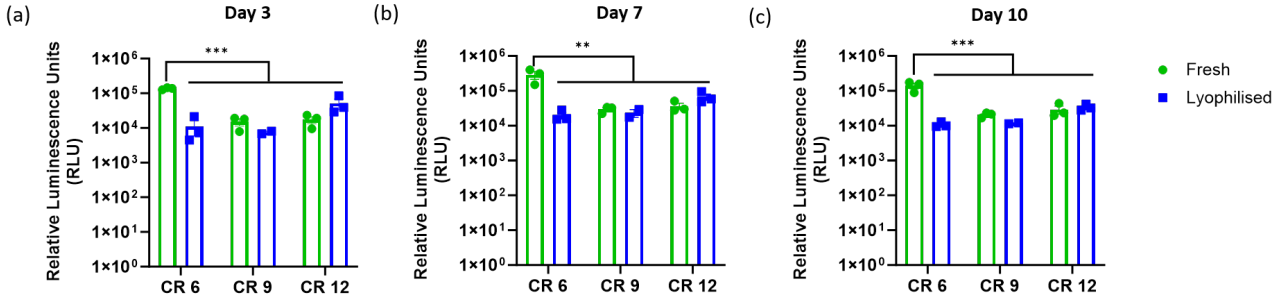

Fig. 4. pDNA expression following transfection with lyophilised GET-pDNA NPs following <7 days storage at room temperature. Freshly complexed NPs at CR 6 demonstrated significantly higher pGLuc expression than all other groups at (**a**) 3 days, (**b**) 7 days and (**c**) 10 days post-transfection, however there was no significant difference in pGLuc expression between freshly complexed and lyophilised NPs at CR 9 or CR 12. Error bars represent ± SE, $n = 3$ repeats. (**) denotes significance, $p < 0.01$. (***) denotes significance $p < 0.001$. pGLuc, plasmids containing the *Gaussia luciferase*.

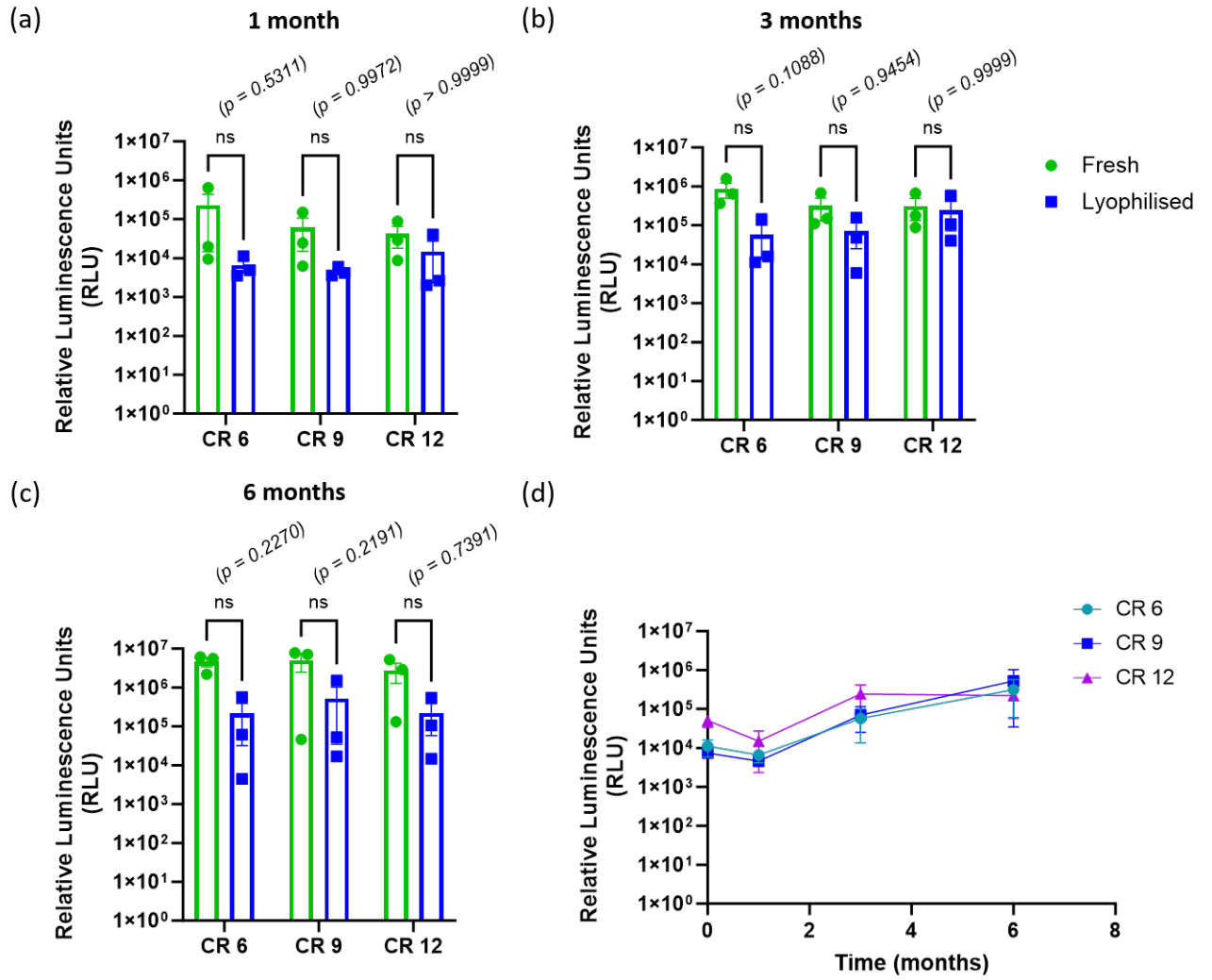

Fig. 5. pDNA expression following transfection with lyophilised GET-pDNA NPs after long-term storage. There was no statistically significant difference in pGLuc expression between freshly complexed and lyophilised NPs at CR 6, 9 or 12 3 days post-transfection following storage at room temperature for (**a**) 1 month, (**b**) 3 months and (**c**) 6 months respectively. (**d**) Lyophilised NPs at CR 6, 9 and 12 maintained steady pGLuc expression following storage at room temperature for up to 6 months. Error bars represent ± SE, $n = 3$ repeats. (ns) denotes no statistical significance.

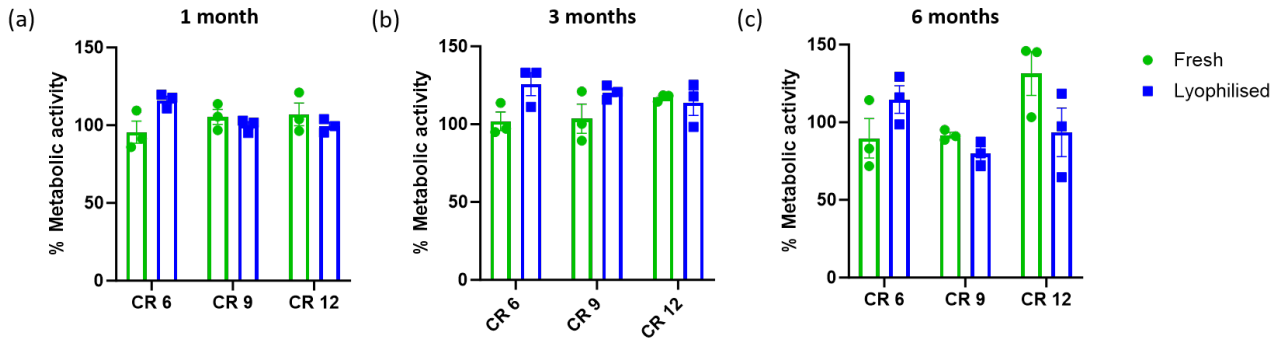

Fig. 6. Cell metabolic activity of MSCs post-transfection with lyophilised GET-pDNA NPs which have been stored for up to 6 months at room temperature. There was no statistically significant difference in cell metabolic activity, normalised to non-treated cell controls, between cells transfected with freshly complexed and lyophilised NPs 3 days post-transfection following storage of the NPs for (**a**) 1 month, (**b**) 3 months and (**c**) 6 months respectively. This indicates that the NPs are non-toxic to the cells. Error bars represent ± SE, $n = 3$ repeats.

Transfection with Lyophilised GET-pDNA Nanoparticles Does not Affect Cell Metabolic Activity

Cell metabolic activity was measured as an indicator of cell viability at 3, 7 and 10 days post-transfection with freshly complexed and lyophilised NPs (Fig. 3). Metabolic activity of the transfected cells was expressed as a percentage of that of the non-treated cell controls. There was no significant difference in MSC metabolic activity following transfection with freshly complexed or lyophilised NPs at all CRs. This finding was mirrored at each respective timepoint.

Transfection with Lyophilised GET-pDNA Nanoparticles Results in Stable Transgene Expression

MSCs were transfected with freshly complexed and lyophilised GET-pGLuc NPs to determine if the lyophilisation process affected the expression of pGLuc (Fig. 4**a**-**c**). There was significantly higher luciferase expression in cells transfected with freshly complexed NPs at CR 6 3, 7 and 10 days post-transfection respectively. However, there was no significant difference in luciferase expression between freshly complexed and lyophilised NP groups at CR 9 and CR 12.

Lyophilised Nanoparticles Maintain Stable Transgene Expression Following Long-Term Storage

To determine if the formulated lyophilised NPs could be stored for prolonged periods of time without affecting transgene expression, MSCs were transfected with lyophilised GET-pGLuc NPs that had been stored at room temperature for 1, 3 and 6 months respectively (Fig. 5). The results were compared against freshly complexed NP controls and lyophilised NPs that were used to transfect MSCs within 7 days of lyophilisation, 72hrs post-transfection. There was no statistically significant difference in transgene expression between lyophilised and freshly complexed NPs at each CR (Fig. 5**a**-**c**) and the lyophilised NPs retained steady levels of transgene expression over the 6 month study period (Fig. 5**d**).

Transfection with Lyophilised GET-pDNA Nanoparticles Does not Affect Cell Metabolic Activity

Cell metabolic activity was measured 3 days post-transfection with freshly complexed and lyophilised NPs which had been stored at room temperature for up to 6 months and was used as an indicator of cell viability (Fig. 6). Metabolic activity of the transfected cells was expressed as a percentage of that of the non-treated cell controls. There was no significant difference in MSC metabolic activity following transfection with freshly complexed or lyophilised NPs at all CRs. This finding was mirrored following transfection with lyophilised NPs that had been stored at room temperature for 1 month, 3 months and 6 months respectively.

Lyophilised GET-pSOX9 Nanoparticles Enhance Sulfated Glycosaminoglycan Deposition by MSCs

To highlight the translational potential of this technology, the ability of 'off-the-shelf' SOX9 gene therapeutic NPs to enhance cell-mediated articular matrix deposition in MeHA-Col II injectable hydrogel scaffolds was assessed following 28 days in culture (Fig. 7). Similar levels of sGAGs were deposited in non-treated and freshly complexed GET-pSOX9 activated hydrogel scaffolds, and moderately increased levels were deposited in lyophilised GET-pSOX9 activated hydrogel scaffolds (Fig. 7**a**). However, quantification of DNA per scaffold showed significantly higher DNA levels in the non-treated group versus the freshly complexed and lyophilised NP treatment groups (Fig. 7**b**). When sGAG deposition was normalised to the DNA content of the scaffolds, it was found that the MSCs which had been pre-transfected with lyophilised GET-pSOX9 NPs deposited significantly higher levels of sGAGs than those that had received no treatment (Fig.

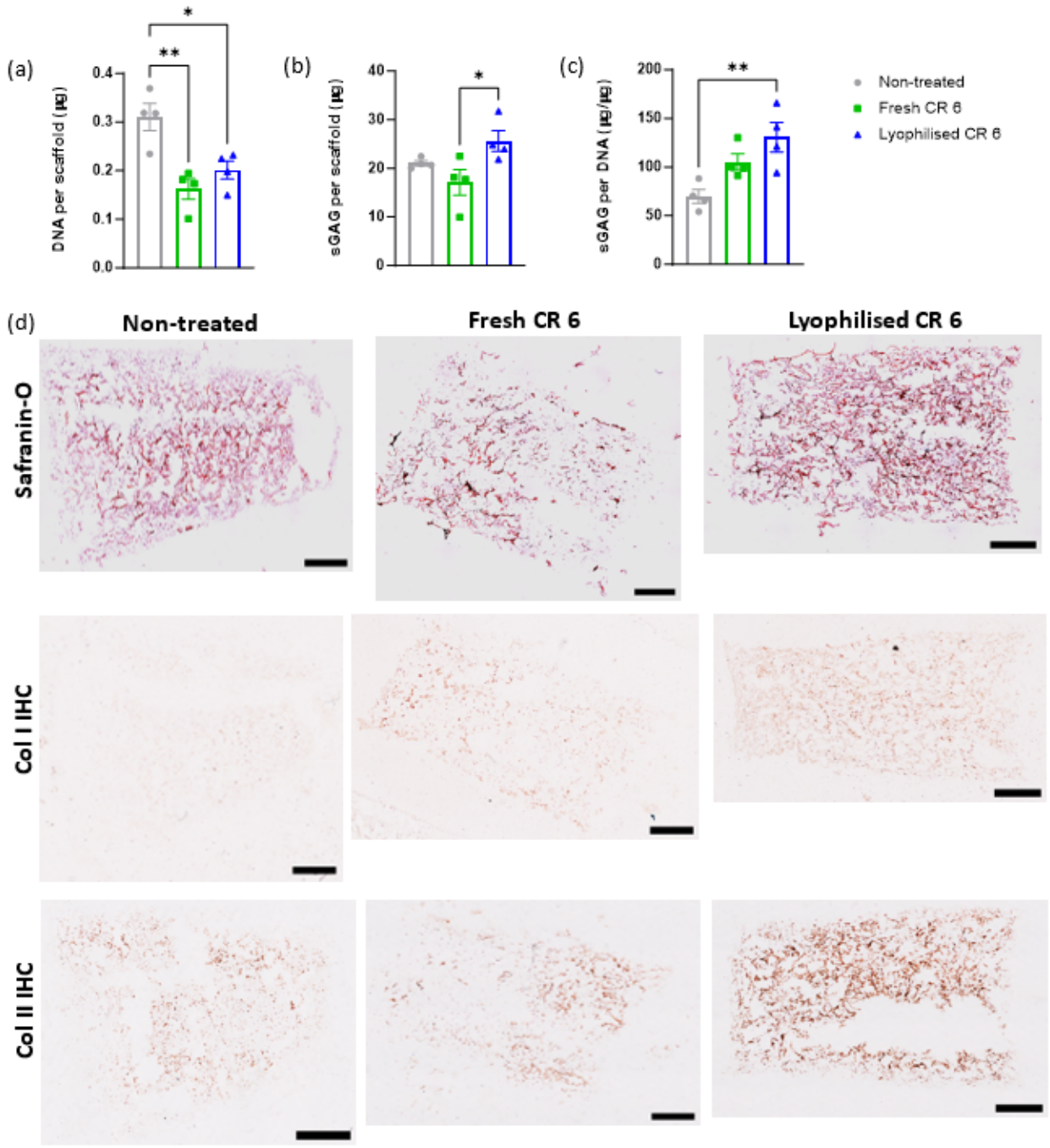

Fig. 7. Matrix deposition by MSCs in hydrogel scaffolds following transfection with freshly complexed or lyophilised GET-pSOX9 NPs. (**a**) A significant increase in sGAG per scaffold was detected in the lyophilised GET-pSOX9-activated scaffolds, while (**b**) significantly higher DNA per scaffold was measured in the non-treated hydrogels versus the gene-activated hydrogels. (**c**) When normalised to DNA, it was found that treatment with lyophilised GET-pSOX9 NPs resulted in significantly higher levels of sGAG deposition versus the non-treated group. (**d**) Safranin-O staining (stains sGAGs red), Col I IHC (stains Col I brown) and Col II IHC (stains Col II brown) showed enhanced articular matrix deposition by MSCs in the lyophilised NP treated scaffolds, with low levels of Col I deposition observed (Scale bar = 1000 µm). Error bars represent ± SE, $n = 4$ scaffolds. (*) denotes significance, $p < 0.05$. (**) denotes significance, $p < 0.01$. sGAG, sulfated glycosaminoglycan; Col I, collagen type I.

7**c**). These results were verified by safranin-O staining (stains sGAGs red), which also showed that sGAG deposition occurred evenly throughout the gene-activated scaffolds. Additionally, Col I and Col II IHC staining showed that transfection with lyophilised GET-pSOX9 NPs resulted in markedly enhanced deposition of Col II by MSCs in the hydrogel scaffolds, with low levels of Col I deposition observed (Fig. 7**d**).

Discussion

This study aimed to investigate lyophilisation as a process to enable stable storage of GET-pDNA nanoparticles (NPs) as an 'off-the-shelf' formulation for use in regenerative medicine applications, with a particular focus on cartilage repair. Firstly, lyophilisation did not affect NP size, polydispersity or surface charge. Next, it was shown that while transfection with freshly complexed NPs at CR 6 resulted in higher levels of pDNA expression, the lyophilised NPs at each CR could still promote stable expression of the pDNA cargo. It was also found that this expression could be sustained following storage of the NPs at room temperature for up to 6 months. Finally, this process of formulating 'off-the-shelf' NPs was shown to have therapeutic applications in the field of regenerative medicine for AC repair. Gene-activation of a MeHA-Col II injectable hydrogel with pro-chondrogenic lyophilised GET-pSOX9 NPs resulted in enhanced MSC-mediated AC matrix synthesis.

The first key finding of this study is that the lyophilised NPs did not differ significantly from freshly complexed NPs in terms of physicochemical properties. This finding is critical as NP size and polydispersity are key factors in determining cellular uptake, influencing both if and how the NP enters the cell (Verma and Stellaci, 2010). Previous studies have shown that NPs in the size range of 50-200 nm, similar to those formulated in this study, are optimal for cellular uptake (Mailänder and Landfester, 2009; Xu *et al.*, 2012). The mean hydrodynamic diameter of the NPs formulated in this study (approx. 120-180 nm) also aligns with values reported in previous studies, where the GET peptide was used as a non-viral vector for pDNA delivery (Power *et al.*, 2022; Raftery *et al.*, 2019). Similarly, NP surface charge is also a key determinant of cellular uptake. Of note, it has been shown that positively charged NPs, such as the GET-pDNA NPs investigated in this study, display improved cellular uptake in a surface charge-dependent manner compared to those with a negative charge (Augustine *et al.*, 2020; He *et al.*, 2010). This is particularly important in cartilage repair where positively charged NPs and drugs have demonstrated enhanced retention in and movement throughout the negatively charged extracellular matrix of AC (Bajpayee and Grodzinsky, 2017). Thus, it is critical that the NPs maintain their positive charge following lyophilisation, which has been successfully demonstrated in this study. Similar to the hydrodynamic diameter of the NPs, the surface charge values observed in this study are also largely in agreement with previous studies conducted using GET-pDNA NPs (Power *et al.*, 2022; Raftery *et al.*, 2019). More than 98 % of pDNA also remained encapsulated within the NPs post-lyophilisation, which indicates that the lyophilisation process did not compromise the structural integrity of the NP. It is important to note is that, in this study, the physicochemical properties of the NPs were preserved during the lyophilisation process using minimal additional excipients. Trehalose was the only excipient added to the formulation which has a generally recognised as safe (GRAS) status assigned to it by the United States Food and Drug Administration (US FDA) (Richards *et al.*, 2002), thus simplifying the potential regulatory approval pathway for this process of formulating 'off-the-shelf' therapeutic NPs.

The second key finding of this study is that transfection with the lyophilised NPs resulted in stable expression of the pDNA cargo at all CRs with no impact on cell viability. In addition, when assessing the gene expression of the lyophilised GET-pDNA NPs following storage at room temperature for up to 6 months, it was found that NPs formulated at higher CRs demonstrated equivalent expression of the pDNA cargo to freshly complexed NP controls at the same CR. These results are significant as one of the major barriers to clinical translation of non-viral delivery systems for gene therapeutics is their instability in aqueous formulations (Sainz-Ramos *et al.*, 2021). Traditionally, in studies investigating these delivery systems, emphasis was often placed on designing vectors with improved transfection efficiency and not on how these gene therapeutic delivery systems might be formulated as a stable marketable product for use in a clinical setting (Copolovici *et al.*, 2014). However, since the development of mRNA-based lipid vaccines against the SARS-CoV-2 (COVID-19) virus by pharmaceutical companies such as Pfizer/BioNTech and Moderna (Baden *et al.*, 2021; Polack *et al.*, 2020), interest has grown in enhancing formulation design for lipid-based non-viral delivery systems for nucleic acid therapeutics (Li *et al.*, 2022; Meulewaeter *et al.*, 2023; Muramatsu *et al.*, 2022). However, studies investigating the development of 'off-the-shelf' gene delivery systems using CPP, inorganic NP or polymer-based vectors are more limited. For example, McErlean *et al.* (2021) developed a lyophilised linear CPP (termed *CHAT*) and pDNA NP formulation that remained stable following 28 days storage at room temperature (McErlean *et al.*, 2021). Likewise, Hosseinpour *et al.* (2021) formulated lyophilised PEI coated mesoporous silica and microRNA-26a-5p NPs, which were shown to successfully enhance osteogenic differentiation of MSCs (Hosseinpour *et al.*, 2021). Similar to this study, each of these studies also used lyophilisation to formulate 'off-the-shelf' NP formulations with a disaccharide cryoprotectant such as trehalose or mannitol, and found that NP physicochemical properties and transgene expression were not adversely affected by the process.

The developed 'off-the-shelf' GET-pSOX9 NPs were also shown to have therapeutic applications in the field of regenerative medicine for cartilage repair, through enhancement of the chondrogenic potential of a previously developed MeHA-Col II injectable hydrogel implant. Gene-activation of the MeHA-Col II injectable hydrogel scaffolds resulted in the production of a sGAG and Col II-rich matrix by MSCs with little to no evidence of fibrocartilage formation, reflecting the composition of native AC.

The SOX family of transcription factors (SOX5, SOX6 and SOX9) have previously been shown to be master regulators of cartilage formation (Green *et al.*, 2015), and so they have become popular targets in the field of regenerative medicine for cartilage repair. While previous studies have demonstrated the regenerative potential of pSOX9 delivery, amongst other pro-chondrogenic nucleic acids, via traditional biomaterial scaffolds (Chen *et al.*, 2011; Cucchiarini and Madry, 2019; Im *et al.*, 2011; Intini *et al.*, 2023; Lee *et al.*, 2017; Madry *et al.*, 2020b; Raftery *et al.*, 2020; Venkatesan *et al.*, 2018), literature on the development of gene-activated hydrogels is limited. In our own lab, Gonzalez *et al.* (2019) developed an alginate-methylcellulose bioink, which was gene-activated with pBMP-2 or a combination of pBMP-2, pTGF-β3 and pSOX9 to formulate osteogenic and chondrogenic bioinks respectively (Gonzalez-Fernandez *et al.*, 2019). Bi-layered osteochondral scaffolds 3D printed using these bioinks were shown to promote the formation of vascularised bone tissue overlaid by articular-like cartilage tissue *in vivo*. Madry *et al.* (2020a) developed an injectable hydrogel based on poly(ethylene oxide) (PEO)-poly(propylene oxide) (PPO)-PEO poloxamers that could be used to deliver recombinant adeno-associated viral (rAAV) vector and pSOX9 NPs *in vivo* for the repair of full thickness chondral defects (Madry *et al.*, 2020a). Similarly, Lolli *et al.* (2019) gene-activated an injectable fibrin/hyaluronan hydrogel with lipofectamine and antagomiR-221 NPs, which was subsequently shown to significantly enhance tissue repair by endogenous cells in an *in vivo* osteochondral defect model (Lolli *et al.*, 2019). However, none of the aforementioned studies used an 'off-the-shelf' gene therapeutic formulation to functionalise the biomaterial scaffold or hydrogel, which potentially complicates the fabrication process. Thus, this study represents a promising development for the clinical translation and potential scale-up of gene-activated biomaterials for cartilage repair, as well as a myriad of other applications.

Of note concerning the design of this study, it was decided not to employ a gold standard non-viral delivery vector such as Lipofectamine® 3000 as a control when investigating the transfection efficiency of the GET-pDNA NPs. This is due to the fact that equivalence between the two vectors has previously been demonstrated by our research group (Raftery *et al.*, 2019). The transfection experiments in this study were also carried out using rat MSCs alone and so a further study will be required in the future using human MSCs to ensure that results observed here are clinically translatable. Regardless, the findings above pave the way for developing an 'off-the-shelf' gene therapeutic using an efficacious and versatile non-viral delivery vector with a good safety profile. The 'off-the-shelf' gene therapeutic can be incorporated into scaffolds or hydrogels for regenerative medicine applications, thus facilitating fabrication of gene-activated living tissue implants for tissue repair. Lyophilisation would allow therapeutic NPs to be prepared in advance and undergo GMP-standard quality checks prior to patient administration to ensure that each batch is consistent, efficacious and safe. Lyophilisation also streamlines the gene-activated scaffold fabrication process, allowing clinicians or technicians to easily reconstitute the therapeutic and add it to tissue engineered scaffolds or hydrogels at the point of use.

Conclusion

In conclusion, this study outlines an effective method for formulating non-viral delivery vector and pDNA therapeutic nanoparticles as 'off-the-shelf' formulations for regenerative medicine applications. However, these findings when taken in isolation also hold potential in advancing the development of a method to formulate and enable long-term, stable storage of gene therapeutics. This will be a key consideration for facilitating clinical translation of gene therapy treatments, for regenerative medicine purposes or otherwise, in the future. A reproducible production process will also help to ensure batch-to-batch uniformity when formulating therapeutic NPs for clinical use, paving the way for larger scale production of these types of therapeutics.

List of Abbreviations

NPs, nanoparticles; AC, Articular cartilage; MSCs, mesenchymal stem cells; HA, hyaluronic acid; Col II, collagen type II; TGF-β, transforming growth factor beta; BMP, bone morphogenetic protein; pDNA, plasmid DNA; CPPs, cell-penetrating peptides; GET, glycosaminoglycan enhanced transduction; FGF2, fibroblast growth factor 2; GMP, good manufacturing practice; SOX9, sex-determining region Y-box 9; CMV, cytomegalovirus; MGH_2O, molecular grade water; dsDNA, double-stranded DNA; DMEM, Dulbeccos's Modified Eagle Medium; FBS, foetal bovine serum; TE, tris-EDTA; MeHA, Methacrylated hyaluronic acid; HA, hyaluronic acid; DMF, N,N-dimethlyformamide; MA, Methacrylic anhydride; NaOH, sodium hydroxide; NaCl, sodium chloride; LAP, Lithium phenyl-2,4,6-trimethylbenzoylphosphinate; PBS, phosphate buffered saline; ICM, incomplete chondrogenic medium; ITS-X, insulin-transferrin-selenium-ethanolamine; CCM, complete chondrogenic medium; sGAG, sulfated glycosaminoglycan; EDTA, ethylenediaminetetraacetic acid; dsDNA, double-stranded DNA; DAB, 3,3′-diaminobenzidine; PdI, Polydispersity index; pGLuc, plasmid DNA containing the *Gaussia luciferase*; PEO, poly(ethylene oxide); PPO, poly(propylene oxide); OCT, optimal cutting temperature; IHC, immunohistochemistry; ANOVA, analysis of variance; CR, charge ratio.

Availability of Data and Materials

Data and materials are available upon reasonable request from the corresponding author.

Author Contributions

DOS, TH, CC and FOB devised the experimental plan for this study, and DOS and TH carried out the experimental work. JD synthesised and provided the GET peptide used in this study. DOS, TH, CC and FOB devised the structure of the manuscript, and DOS drafted and wrote the manuscript. DOS created figures used unless otherwise stated. DOS, TH, JD, CC, and FOB revised the manuscript critically and suggested references. CC and FOB supervised the project and FOB provided funding for the project. All authors have read and approved the final submitted manuscript.

Ethics Approval and Consent to Participate

This study was approved by the Research Ethics Committee of the Royal College of Surgeons in Ireland under application number REC202012003.

Acknowledgments

All original figures were created with Biorender.com.

Funding

The authors acknowledge funding from the European Research Council under the European Community's Horizon 2020 research and innovation programme under ERC Advanced Grant agreement n° 788753 (ReCaP). Dr. Curtin acknowledges funding from the Health Research Board (HRB) in Ireland under grant agreement ILP-POR-2019-023. Dr. Hodgkinson acknowledges funding from Science Foundation Ireland (SFI) under Grant number: 21/PATH-S/9306.

Conflict of Interest

The authors declare no conflict of interest. FJO is serving the Editorial Board members of this journal. We declare that FJO had no involvement in the peer review of this article and has no access to information regarding its peer review. Full responsibility for the editorial process for this article was delegated to MS.

References

Augustine R, Hasan A, Primavera R, Wilson RJ, Thakor AS, Kevadiya BD (2020) Cellular uptake and retention of nanoparticles: Insights on particle properties and interaction with cellular components. Materials Today Communications 25: 101692. DOI: 10.1016/j.mtcomm.2020.101692.

Baden LR, El Sahly HM, Essink B, Kotloff K, Frey S, Novak R, Diemert D, Spector SA, Rouphael N, Creech CB, McGettigan J, Khetan S, Segall N, Solis J, Brosz A, Fierro C, Schwartz H, Neuzil K, Corey L, Gilbert P, Janes H, Follmann D, Marovich M, Mascola J, Polakowski L, Ledgerwood J, Graham BS, Bennett H, Pajon R, Knightly C, Leav B, Deng W, Zhou H, Han S, Ivarsson M, Miller J, Zaks T, COVE Study Group (2021) Efficacy and Safety of the mRNA-1273 SARS-CoV-2 Vaccine. The New England Journal of Medicine 384: 403-416. DOI: 10.1056/NEJMoa2035389.

Bajpayee AG, Grodzinsky AJ (2017) Cartilage-targeting drug delivery: can electrostatic interactions help? Nature Reviews. Rheumatology 13: 183-193. DOI: 10.1038/nrrheum.2016.210.

Ball RL, Bajaj P, Whitehead KA (2017) Achieving long-term stability of lipid nanoparticles: examining the effect of pH, temperature, and lyophilization. International Journal of Nanomedicine 12: 305-315. DOI: 10.2147/IJN.S123062.

Biondi M, Ungaro F, Quaglia F, Netti PA (2008) Controlled drug delivery in tissue engineering. Advanced Drug Delivery Reviews 60: 229-242. DOI: 10.1016/j.addr.2007.08.038.

Bjelošević M, Zvonar Pobirk A, Planinšek O, Ahlin Grabnar P (2020) Excipients in freeze-dried biopharmaceuticals: Contributions toward formulation stability and lyophilisation cycle optimisation. International Journal of Pharmaceutics 576: 119029. DOI: 10.1016/j.ijpharm.2020.119029.

Bleiziffer O, Eriksson E, Yao F, Horch RE, Kneser U (2007) Gene transfer strategies in tissue engineering. Journal of Cellular and Molecular Medicine 11: 206-223. DOI: 10.1111/j.1582-4934.2007.00027.x.

Bulaklak K, Gersbach CA (2020) The once and future gene therapy. Nature Communications 11: 5820. DOI: 10.1038/s41467-020-19505-2.

Chen FM, Zhang M, Wu ZF (2010) Toward delivery of multiple growth factors in tissue engineering. Biomaterials 31: 6279-6308. DOI: 10.1016/j.biomaterials.2010.04.053.

Chen J, Chen H, Li P, Diao H, Zhu S, Dong L, Wang R, Guo T, Zhao J, Zhang J (2011) Simultaneous regeneration of articular cartilage and subchondral bone in vivo using MSCs induced by a spatially controlled gene delivery system in bilayered integrated scaffolds. Biomaterials 32: 4793-4805. DOI: 10.1016/j.biomaterials.2011.03.041.

Chen L, Liu J, Guan M, Zhou T, Duan X, Xiang Z (2020) Growth Factor and Its Polymer Scaffold-Based Delivery System for Cartilage Tissue Engineering. International Journal of Nanomedicine 15: 6097-6111. DOI: 10.2147/IJN.S249829.

Chen L, Zhang J, Wang J, Lin J, Luo X, Cui W (2023) Inflammation-Regulated Auto Aggregated Hydrogel Microspheres Via Anchoring Cartilage Deep Matrix for Genes Delivery. Advanced Functional Materials 33: 2305635. DOI: 10.1002/adfm.202305635.

Cole G, Ali AA, McCrudden CM, McBride JW, McCaffrey J, Robson T, Kett VL, Dunne NJ, Donnelly RF, McCarthy HO (2018) DNA vaccination for cervical cancer: Strategic optimisation of RALA mediated gene delivery from a biodegradable microneedle system. European Journal of Pharmaceutics and Biopharmaceutics: Official Journal of Arbeitsgemeinschaft Fur Phar-

mazeutische Verfahrenstechnik E.V 127: 288-297. DOI: 10.1016/j.ejpb.2018.02.029.

Collins KH, Pferdehirt L, Saleh LS, Savadipour A, Springer LE, Lenz KL, Thompson DM, Jr, Oswald SJ, Pham CTN, Guilak F (2023) Hydrogel Encapsulation of Genome-Engineered Stem Cells for Long-Term Self-Regulating Anti-Cytokine Therapy. Gels (Basel, Switzerland) 9: 169. DOI: 10.3390/gels9020169.

Copolovici DM, Langel K, Eriste E, Langel Ü (2014) Cell-penetrating peptides: design, synthesis, and applications. ACS Nano 8: 1972-1994. DOI: 10.1021/nn4057269.

Cucchiarini M, Madry H (2019) Biomaterial-guided delivery of gene vectors for targeted articular cartilage repair. Nature Reviews. Rheumatology 15: 18-29. DOI: 10.1038/s41584-018-0125-2.

Curtin CM, Tierney EG, McSorley K, Cryan SA, Duffy GP, O'Brien FJ (2015) Combinatorial gene therapy accelerates bone regeneration: non-viral dual delivery of VEGF and BMP2 in a collagen-nanohydroxyapatite scaffold. Advanced Healthcare Materials 4: 223-227. DOI: 10.1002/adhm.201400397.

Danaei M, Dehghankhold M, Ataei S, Hasanzadeh Davarani F, Javanmard R, Dokhani A, Khorasani S, Mozafari MR (2018) Impact of Particle Size and Polydispersity Index on the Clinical Applications of Lipidic Nanocarrier Systems. Pharmaceutics 10: 57. DOI: 10.3390/pharmaceutics10020057.

Dixon JE, Osman G, Morris GE, Markides H, Rotherham M, Bayoussef Z, El Haj AJ, Denning C, Shakesheff KM (2016) Highly efficient delivery of functional cargoes by the synergistic effect of GAG binding motifs and cell-penetrating peptides. Proceedings of the National Academy of Sciences of the United States of America 113: E291-9. DOI: 10.1073/pnas.1518634113.

Dixon JE, Wellington V, Elnima A, Eltaher HM (2024) Effects of Microenvironment and Dosing on Efficiency of Enhanced Cell Penetrating Peptide Nonviral Gene Delivery. ACS Omega 9: 5014-5023. DOI: 10.1021/acsomega.3c09306.

Dunbar CE, High KA, Joung JK, Kohn DB, Ozawa K, Sadelain M (2018) Gene therapy comes of age. Science (New York, N.Y.) 359: eaan4672. DOI: 10.1126/science.aan4672.

Erickson IE, Huang AH, Sengupta S, Kestle S, Burdick JA, Mauck RL (2009) Macromer density influences mesenchymal stem cell chondrogenesis and maturation in photocrosslinked hyaluronic acid hydrogels. Osteoarthritis and Cartilage 17: 1639-1648. DOI: 10.1016/j.joca.2009.07.003.

Freeman FE, Pitacco P, van Dommelen LHA, Nulty J, Browe DC, Shin JY, Alsberg E, Kelly DJ (2020) 3D bioprinting spatiotemporally defined patterns of growth factors to tightly control tissue regeneration. Science Advances 6: eabb5093. DOI: 10.1126/sciadv.abb5093.

Gonzalez-Fernandez T, Rathan S, Hobbs C, Pitacco P, Freeman FE, Cunniffe GM, Dunne NJ, McCarthy HO, Nicolosi V, O'Brien FJ, Kelly DJ (2019) Pore-forming bioinks to enable spatio-temporally defined gene delivery in bioprinted tissues. Journal of Controlled Release: Official Journal of the Controlled Release Society 301: 13-27. DOI: 10.1016/j.jconrel.2019.03.006.

Gonzalez-Fernandez T, Tierney EG, Cunniffe GM, O'Brien FJ, Kelly DJ (2016) Gene Delivery of TGF-β3 and BMP2 in an MSC-Laden Alginate Hydrogel for Articular Cartilage and Endochondral Bone Tissue Engineering. Tissue Engineering. Part a 22: 776-787. DOI: 10.1089/ten.TEA.2015.0576.

Green JD, Tollemar V, Dougherty M, Yan Z, Yin L, Ye J, Collier Z, Mohammed MK, Haydon RC, Luu HH, Kang R, Lee MJ, Ho SH, He TC, Shi LL, Athiviraham A (2015) Multifaceted signaling regulators of chondrogenesis: Implications in cartilage regeneration and tissue engineering. Genes & Diseases 2: 307-327. DOI: 10.1016/j.gendis.2015.09.003.

Guo X, Huang L (2012) Recent advances in nonviral vectors for gene delivery. Accounts of Chemical Research 45: 971-979. DOI: 10.1021/ar200151m.

Hahn LD, Kong H, Mooney DJ (2010) Polycation structure mediates expression of lyophilized polycation/pDNA complexes. Macromolecular Bioscience 10: 1210-1215. DOI: 10.1002/mabi.201000067.

Hamm A, Krott N, Breibach I, Blindt R, Bosserhoff AK (2002) Efficient transfection method for primary cells. Tissue Engineering 8: 235-245. DOI: 10.1089/107632702753725003.

Hauptstein J, Böck T, Bartolf-Kopp M, Forster L, Stahlhut P, Nadernezhad A, Blahetek G, Zernecke-Madsen A, Detsch R, Jüngst T, Groll J, Teßmar J, Blunk T (2020) Hyaluronic Acid-Based Bioink Composition Enabling 3D Bioprinting and Improving Quality of Deposited Cartilaginous Extracellular Matrix. Advanced Healthcare Materials 9: e2000737. DOI: 10.1002/adhm.202000737.

Hauptstein J, Forster L, Nadernezhad A, Groll J, Teßmar J, Blunk T (2022) Tethered TGF-β1 in a Hyaluronic Acid-Based Bioink for Bioprinting Cartilaginous Tissues. International Journal of Molecular Sciences 23: 924. DOI: 10.3390/ijms23020924.

He C, Hu Y, Yin L, Tang C, Yin C (2010) Effects of particle size and surface charge on cellular uptake and biodistribution of polymeric nanoparticles. Biomaterials 31: 3657-3666. DOI: 10.1016/j.biomaterials.2010.01.065.

Hodgkinson T, Amado IN, O'Brien FJ, Kennedy OD (2022a) The role of mechanobiology in bone and cartilage model systems in characterizing initiation and progression of osteoarthritis. APL Bioengineering 6. DOI: 10.1063/5.0068277.

Hodgkinson T, Kelly DC, Curtin CM, O'Brien FJ (2022b) Mechanosignalling in cartilage: an emerging target for the treatment of osteoarthritis. Nature Reviews. Rheumatology 18: 67-84. DOI: 10.1038/s41584-021-

00724-w.

Hosseinpour S, Cao Y, Liu J, Xu C, Walsh LJ (2021) Efficient transfection and long-term stability of rno-miRNA-26a-5p for osteogenic differentiation by large pore sized mesoporous silica nanoparticles. Journal of Materials Chemistry. B 9: 2275-2284. DOI: 10.1039/d0tb02756a.

Im GI, Kim HJ, Lee JH (2011) Chondrogenesis of adipose stem cells in a porous PLGA scaffold impregnated with plasmid DNA containing SOX trio (SOX-5,-6 and -9) genes. Biomaterials 32: 4385-4392. DOI: 10.1016/j.biomaterials.2011.02.054.

Intini C, Blokpoel Ferreras L, Casey S, Dixon JE, Gleeson JP, O'Brien FJ (2023) An Innovative miR-Activated Scaffold for the Delivery of a miR-221 Inhibitor to Enhance Cartilage Defect Repair. Advanced Therapeutics 6: 2200329. DOI: 10.1002/adtp.202200329.

Intini C, Hodgkinson T, Casey SM, Gleeson JP, O'Brien FJ (2022a) Highly Porous Type II Collagen-Containing Scaffolds for Enhanced Cartilage Repair with Reduced Hypertrophic Cartilage Formation. Bioengineering (Basel, Switzerland) 9: 232. DOI: 10.3390/bioengineering9060232.

Intini C, Lemoine M, Hodgkinson T, Casey S, Gleeson JP, O'Brien FJ (2022b) A highly porous type II collagen containing scaffold for the treatment of cartilage defects enhances MSC chondrogenesis and early cartilaginous matrix deposition. Biomaterials Science 10: 970-983. DOI: 10.1039/d1bm01417j.

Jeon SY, Park JS, Yang HN, Woo DG, Park KH (2012) Co-delivery of SOX9 genes and anti-Cbfa-1 siRNA coated onto PLGA nanoparticles for chondrogenesis of human MSCs. Biomaterials 33: 4413-4423. DOI: 10.1016/j.biomaterials.2012.02.051.

Joyce M, Hodgkinson T, Intini C, Dixon JE, Kelly DJ, O'Brien FJ (2024) Gene activated reinforced scaffolds for SOX9 delivery to enhance repair of large load bearing articular cartilage defects. European Cells and Materials 47: 91-108. DOI: 10.22203/eCM.v047a07.

Joyce M, Hodgkinson T, Lemoine M, González-Vázquez A, Kelly DJ, O'Brien FJ (2023) Development of a 3D-printed bioabsorbable composite scaffold with mechanical properties suitable for treating large, load-bearingarticular cartilage defects. European Cells & Materials 45: 158-172. DOI: 10.22203/eCM.v045a11.

Kajave NS, Schmitt T, Nguyen TU, Kishore V (2020) Dual crosslinking strategy to generate mechanically viable cell-laden printable constructs using methacrylated collagen bioinks. Materials Science & Engineering. C, Materials for Biological Applications 107: 110290. DOI: 10.1016/j.msec.2019.110290.

Keil TWM, Feldmann DP, Costabile G, Zhong Q, da Rocha S, Merkel OM (2019) Characterization of spray dried powders with nucleic acid-containing PEI nanoparticles. European Journal of Pharmaceutics and Biopharmaceutics: Official Journal of Arbeitsgemeinschaft Fur Pharmazeutische Verfahrenstechnik E.V 143: 61-69. DOI: 10.1016/j.ejpb.2019.08.012.

Kelly DC, Raftery RM, Curtin CM, O'Driscoll CM, O'Brien FJ (2019) Scaffold-Based Delivery of Nucleic Acid Therapeutics for Enhanced Bone and Cartilage Repair. Journal of Orthopaedic Research: Official Publication of the Orthopaedic Research Society 37: 1671-1680. DOI: 10.1002/jor.24321.

Kilmer CE, Battistoni CM, Cox A, Breur GJ, Panitch A, Liu JC (2020) Collagen Type I and II Blend Hydrogel with Autologous Mesenchymal Stem Cells as a Scaffold for Articular Cartilage Defect Repair. ACS Biomaterials Science & Engineering 6: 3464-3476. DOI: 10.1021/acsbiomaterials.9b01939.

Kwon H, Brown WE, Lee CA, Wang D, Paschos N, Hu JC, Athanasiou KA (2019) Surgical and tissue engineering strategies for articular cartilage and meniscus repair. Nature Reviews. Rheumatology 15: 550-570. DOI: 10.1038/s41584-019-0255-1.

Laird NZ, Acri TM, Tingle K, Salem AK (2021) Gene- and RNAi-activated scaffolds for bone tissue engineering: Current progress and future directions. Advanced Drug Delivery Reviews 174: 613-627. DOI: 10.1016/j.addr.2021.05.009.

Lee YH, Wu HC, Yeh CW, Kuan CH, Liao HT, Hsu HC, Tsai JC, Sun JS, Wang TW (2017) Enzyme-crosslinked gene-activated matrix for the induction of mesenchymal stem cells in osteochondral tissue regeneration. Acta Biomaterialia 63: 210-226. DOI: 10.1016/j.actbio.2017.09.008.

Li Z, Zhang XQ, Ho W, Bai X, Jaijyan DK, Li F, Kumar R, Kolloli A, Subbian S, Zhu H, Xu X (2022) Lipid-Polymer Hybrid "Particle-in-Particle" Nanostructure Gene Delivery Platform Explored for Lyophilizable DNA and mRNA COVID-19 Vaccines. Advanced Functional Materials 32: 2204462. DOI: 10.1002/adfm.202204462.

Liang Q, Ma Y, Yao X, Wei W (2022) Advanced 3D-Printing Bioinks for Articular Cartilage Repair. International Journal of Bioprinting 8: 511. DOI: 10.18063/ijb.v8i3.511.

Liu W, Venkatesan JK, Amini M, Oláh T, Schmitt G, Madry H, Cucchiarini M (2023) Effects of rAAV-Mediated Overexpression of sox9 and TGF-ß via Alginate Hydrogel-Guided Vector Delivery on the Chondroreparative Activities of Human Bone Marrow-Derived Mesenchymal Stromal Cells. Journal of Tissue Engineering and Regenerative Medicine 2023: 4495697. DOI: 10.1155/2023/4495697.

Lolli A, Sivasubramaniyan K, Vainieri ML, Oieni J, Kops N, Yayon A, van Osch GJVM (2019) Hydrogel-based delivery of antimiR-221 enhances cartilage regeneration by endogenous cells. Journal of Controlled Release: Official Journal of the Controlled Release Society 309: 220-230. DOI: 10.1016/j.jconrel.2019.07.040.

Luo C, Xie R, Zhang J, Liu Y, Li Z, Zhang Y, Zhang X, Yuan T, Chen Y, Fan W (2020) Low-Temperature Three-

Dimensional Printing of Tissue Cartilage Engineered with Gelatin Methacrylamide. Tissue Engineering. Part C, Methods 26: 306-316. DOI: 10.1089/ten.TEC.2020.0053.

Madry H, Gao L, Rey-Rico A, Venkatesan JK, Müller-Brandt K, Cai X, Goebel L, Schmitt G, Speicher-Mentges S, Zurakowski D, Menger MD, Laschke MW, Cucchiarini M (2020a) Thermosensitive Hydrogel Based on PEO-PPO-PEO Poloxamers for a Controlled In Situ Release of Recombinant Adeno-Associated Viral Vectors for Effective Gene Therapy of Cartilage Defects. Advanced Materials (Deerfield Beach, Fla.) 32: e1906508. DOI: 10.1002/adma.201906508.

Madry H, Venkatesan JK, Carballo-Pedrares N, Rey-Rico A, Cucchiarini M (2020b) Scaffold-Mediated Gene Delivery for Osteochondral Repair. Pharmaceutics 12: 930. DOI: 10.3390/pharmaceutics12100930.

Maihöfer J, Madry H, Rey-Rico A, Venkatesan JK, Goebel L, Schmitt G, Speicher-Mentges S, Cai X, Meng W, Zurakowski D, Menger MD, Laschke MW, Cucchiarini M (2021) Hydrogel-Guided, rAAV-Mediated IGF-I Overexpression Enables Long-Term Cartilage Repair and Protection against Perifocal Osteoarthritis in a Large-Animal Full-Thickness Chondral Defect Model at One Year In Vivo. Advanced Materials (Deerfield Beach, Fla.) 33: e2008451. DOI: 10.1002/adma.202008451.

Mailänder V, Landfester K (2009) Interaction of nanoparticles with cells. Biomacromolecules 10: 2379-2400. DOI: 10.1021/bm900266r.

McErlean EM, Ziminska M, McCrudden CM, McBride JW, Loughran SP, Cole G, Mulholland EJ, Kett V, Buckley NE, Robson T, Dunne NJ, McCarthy HO (2021) Rational design and characterisation of a linear cell penetrating peptide for non-viral gene delivery. Journal of Controlled Release: Official Journal of the Controlled Release Society 330: 1288-1299. DOI: 10.1016/j.jconrel.2020.11.037.

Meulewaeter S, Nuytten G, Cheng MHY, De Smedt SC, Cullis PR, De Beer T, Lentacker I, Verbeke R (2023) Continuous freeze-drying of messenger RNA lipid nanoparticles enables storage at higher temperatures. Journal of Controlled Release: Official Journal of the Controlled Release Society 357: 149-160. DOI: 10.1016/j.jconrel.2023.03.039.

Municoy S, Álvarez Echazú MI, Antezana PE, Galdopórpora JM, Olivetti C, Mebert AM, Foglia ML, Tuttolomondo MV, Alvarez GS, Hardy JG, Desimone MF (2020) Stimuli-Responsive Materials for Tissue Engineering and Drug Delivery. International Journal of Molecular Sciences 21: 4724. DOI: 10.3390/ijms21134724.

Muramatsu H, Lam K, Bajusz C, Laczkó D, Karikó K, Schreiner P, Martin A, Lutwyche P, Heyes J, Pardi N (2022) Lyophilization provides long-term stability for a lipid nanoparticle-formulated, nucleoside-modified mRNA vaccine. Molecular Therapy: the Journal of the American Society of Gene Therapy 30: 1941-1951. DOI: 10.1016/j.ymthe.2022.02.001.

Ni T, Liu M, Zhang Y, Cao Y, Pei R (2020) 3D Bioprinting of Bone Marrow Mesenchymal Stem Cell-Laden Silk Fibroin Double Network Scaffolds for Cartilage Tissue Repair. Bioconjugate Chemistry 31: 1938-1947. DOI: 10.1021/acs.bioconjchem.0c00298.

O'Brien FJ (2011) Biomaterials & scaffolds for tissue engineering. Materials Today 14: 88-95. DOI: 10.1016/S1369-7021(11)70058-X.

O'Shea DG, Curtin CM, O'Brien FJ (2022) Articulation inspired by nature: a review of biomimetic and biologically active 3D printed scaffolds for cartilage tissue engineering. Biomaterials Science 10: 2462-2483. DOI: 10.1039/d1bm01540k.

O'Shea DG, Hodgkinson T, Curtin CM, O'Brien FJ (2024) An injectable and 3D printable pro-chondrogenic hyaluronic acid and collagen type II composite hydrogel for the repair of articular cartilage defects. Biofabrication 16: 10.1088/1758-5090/ad047a. DOI: 10.1088/1758-5090/ad047a.

Osman G, Rodriguez J, Chan SY, Chisholm J, Duncan G, Kim N, Tatler AL, Shakesheff KM, Hanes J, Suk JS, Dixon JE (2018) PEGylated enhanced cell penetrating peptide nanoparticles for lung gene therapy. Journal of Controlled Release: Official Journal of the Controlled Release Society 285: 35-45. DOI: 10.1016/j.jconrel.2018.07.001.

Pelttari K, Lorenz H, Boeuf S, Templin MF, Bischel O, Goetzke K, Hsu HY, Steck E, Richter W (2008) Secretion of matrix metalloproteinase 3 by expanded articular chondrocytes as a predictor of ectopic cartilage formation capacity in vivo. Arthritis and Rheumatism 58: 467-474. DOI: 10.1002/art.23302.

Polack FP, Thomas SJ, Kitchin N, Absalon J, Gurtman A, Lockhart S, Perez JL, Pérez Marc G, Moreira ED, Zerbini C, Bailey R, Swanson KA, Roychoudhury S, Koury K, Li P, Kalina WV, Cooper D, Frenck RW, Jr, Hammitt LL, Türeci Ö, Nell H, Schaefer A, Ünal S, Tresnan DB, Mather S, Dormitzer PR, Şahin U, Jansen KU, Gruber WC, C4591001 Clinical Trial Group (2020) Safety and Efficacy of the BNT162b2 mRNA Covid-19 Vaccine. The New England Journal of Medicine 383: 2603-2615. DOI: 10.1056/NEJMoa2034577.

Power RN, Cavanagh BL, Dixon JE, Curtin CM, O'Brien FJ (2022) Development of a Gene-Activated Scaffold Incorporating Multifunctional Cell-Penetrating Peptides for pSDF-1α Delivery for Enhanced Angiogenesis in Tissue Engineering Applications. International Journal of Molecular Sciences 23: 1460. DOI: 10.3390/ijms23031460.

Puiggalí-Jou A, Asadikorayem M, Maniura-Weber K, Zenobi-Wong M (2023) Growth factor-loaded sulfated microislands in granular hydrogels promote hMSCs migration and chondrogenic differentiation. Acta Biomaterialia 166: 69-84. DOI: 10.1016/j.actbio.2023.03.045.

Raftery RM, Gonzalez Vazquez AG, Chen G, O'Brien

FJ (2020) Activation of the SOX-5, SOX-6, and SOX-9 Trio of Transcription Factors Using a Gene-Activated Scaffold Stimulates Mesenchymal Stromal Cell Chondrogenesis and Inhibits Endochondral Ossification. Advanced Healthcare Materials 9: e1901827. DOI: 10.1002/adhm.201901827.

Raftery RM, Mencía-Castaño I, Sperger S, Chen G, Cavanagh B, Feichtinger GA, Redl H, Hacobian A, O'Brien FJ (2018) Delivery of the improved BMP-2-Advanced plasmid DNA within a gene-activated scaffold accelerates mesenchymal stem cell osteogenesis and critical size defect repair. Journal of Controlled Release: Official Journal of the Controlled Release Society 283: 20-31. DOI: 10.1016/j.jconrel.2018.05.022.

Raftery RM, Walsh DP, Blokpoel Ferreras L, Mencía Castaño I, Chen G, LeMoine M, Osman G, Shakesheff KM, Dixon JE, O'Brien FJ (2019) Highly versatile cell-penetrating peptide loaded scaffold for efficient and localised gene delivery to multiple cell types: From development to application in tissue engineering. Biomaterials 216: 119277. DOI: 10.1016/j.biomaterials.2019.119277.

Richards AB, Krakowka S, Dexter LB, Schmid H, Wolterbeek APM, Waalkens-Berendsen DH, Shigoyuki A, Kurimoto M (2002) Trehalose: a review of properties, history of use and human tolerance, and results of multiple safety studies. Food and Chemical Toxicology: an International Journal Published for the British Industrial Biological Research Association 40: 871-898. DOI: 10.1016/s0278-6915(02)00011-x.

Rilo-Alvarez H, Ledo AM, Vidal A, Garcia-Fuentes M (2021) Delivery of transcription factors as modulators of cell differentiation. Drug Delivery and Translational Research 11: 426-444. DOI: 10.1007/s13346-021-00931-8.

Sainz-Ramos M, Gallego I, Villate-Beitia I, Zarate J, Maldonado I, Puras G, Pedraz JL (2021) How Far Are Non-Viral Vectors to Come of Age and Reach Clinical Translation in Gene Therapy? International Journal of Molecular Sciences 22: 7545. DOI: 10.3390/ijms22147545.

Spiliotopoulos A, Blokpoel Ferreras L, Densham RM, Caulton SG, Maddison BC, Morris JR, Dixon JE, Gough KC, Dreveny I (2019) Discovery of peptide ligands targeting a specific ubiquitin-like domain-binding site in the deubiquitinase USP11. The Journal of Biological Chemistry 294: 424-436. DOI: 10.1074/jbc.RA118.004469.

Steadman JR, Miller BS, Karas SG, Schlegel TF, Briggs KK, Hawkins RJ (2003) The microfracture technique in the treatment of full-thickness chondral lesions of the knee in National Football League players. The Journal of Knee Surgery 16: 83-86.

Thiagarajan L, Abu-Awwad HADM, Dixon JE (2017) Osteogenic Programming of Human Mesenchymal Stem Cells with Highly Efficient Intracellular Delivery of RUNX2. Stem Cells Translational Medicine 6: 2146-2159. DOI: 10.1002/sctm.17-0137.

Trenkenschuh E, Friess W (2021) Freeze-drying of nanoparticles: How to overcome colloidal instability by formulation and process optimization. European Journal of Pharmaceutics and Biopharmaceutics: Official Journal of Arbeitsgemeinschaft Fur Pharmazeutische Verfahrenstechnik E.V 165: 345-360. DOI: 10.1016/j.ejpb.2021.05.024.

U.S. Food and Drug Administration (2018) What is Gene Therapy? Available at: https://www.fda.gov/vaccines-blood-biologics/cellular-gene-therapy-products/what-gene-therapy#footnote1 (Accessed: 11 April 2023).

Veilleux D, Nelea M, Biniecki K, Lavertu M, Buschmann MD (2016) Preparation of Concentrated Chitosan/DNA Nanoparticle Formulations by Lyophilization for Gene Delivery at Clinically Relevant Dosages. Journal of Pharmaceutical Sciences 105: 88-96. DOI: 10.1016/j.xphs.2015.11.001.

Venkatesan JK, Gardner O, Rey-Rico A, Eglin D, Alini M, Stoddart MJ, Cucchiarini M, Madry H (2018) Improved Chondrogenic Differentiation of rAAV SOX9-Modified Human MSCs Seeded in Fibrin-Polyurethane Scaffolds in a Hydrodynamic Environment. International Journal of Molecular Sciences 19: 2635. DOI: 10.3390/ijms19092635.

Verma A, Stellacci F (2010) Effect of surface properties on nanoparticle-cell interactions. Small (Weinheim an Der Bergstrasse, Germany) 6: 12-21. DOI: 10.1002/smll.200901158.

Walsh DP, Raftery RM, Murphy R, Chen G, Heise A, O'Brien FJ, Cryan SA (2021) Gene activated scaffolds incorporating star-shaped polypeptide-pDNA nanomedicines accelerate bone tissue regeneration in vivo. Biomaterials Science 9: 4984-4999. DOI: 10.1039/d1bm00094b.

Wang B, Díaz-Payno PJ, Browe DC, Freeman FE, Nulty J, Burdis R, Kelly DJ (2021) Affinity-bound growth factor within sulfated interpenetrating network bioinks for bioprinting cartilaginous tissues. Acta Biomaterialia 128: 130-142. DOI: 10.1016/j.actbio.2021.04.016.

Xu A, Yao M, Xu G, Ying J, Ma W, Li B, Jin Y (2012) A physical model for the size-dependent cellular uptake of nanoparticles modified with cationic surfactants. International Journal of Nanomedicine 7: 3547-3554. DOI: 10.2147/IJN.S32188.

Yang R, Chen F, Guo J, Zhou D, Luan S (2020) Recent advances in polymeric biomaterials-based gene delivery for cartilage repair. Bioactive Materials 5: 990-1003. DOI: 10.1016/j.bioactmat.2020.06.004.

Yang Z, Zhao T, Gao C, Cao F, Li H, Liao Z, Fu L, Li P, Chen W, Sun Z, Jiang S, Tian Z, Tian G, Zha K, Pan T, Li X, Sui X, Yuan Z, Liu S, Guo Q (2021) 3D-Bioprinted Difunctional Scaffold for In Situ Cartilage Regeneration Based on Aptamer-Directed Cell Recruitment and Growth Factor-Enhanced Cell Chondrogenesis. ACS Applied Materials & Interfaces 13: 23369-23383. DOI: 10.1021/acsami.1c01844.

Yuan L, Li B, Yang J, Ni Y, Teng Y, Guo L, Fan H, Fan

Y, Zhang X (2016) Effects of Composition and Mechanical Property of Injectable Collagen I/II Composite Hydrogels on Chondrocyte Behaviors. Tissue Engineering. Part a 22: 899-906. DOI: 10.1089/ten.TEA.2015.0513.

Zhao P, Hou X, Yan J, Du S, Xue Y, Li W, Xiang G, Dong Y (2020) Long-term storage of lipid-like nanoparticles for mRNA delivery. Bioactive Materials 5: 358-363. DOI: 10.1016/j.bioactmat.2020.03.001.

Editor's note: The Scientific Editor responsible for this paper was Martin Stoddart.